Inorganic Chemistry
Article

Inorg. Chem. **2009**, *48*, 5555–5561 **5555**
DOI: 10.1021/ic900142h

Experimental Evidence for the Participation of 5d Gd^{III} Orbitals in the Magnetic Interaction in Ni−Gd Complexes

Jean-Pierre Costes,*[,†,‡] Tomoka Yamaguchi,[§] Masaaki Kojima,[§] and Laure Vendier[†,‡]

[†]*CNRS, LCC (Laboratoire de Chimie de Coordination), 205, route de Narbonne, F-31077 Toulouse, France,* [‡]*Université de Toulouse, UPS, INPT, LCC, F-31077 Toulouse, France, and* [§]*Department of Chemistry, Faculty of Science, Okayama University, Tsushima-naka 3-1-1, Okayama 700-8530*

Received January 22, 2009

The syntheses, structural determinations, and magnetic studies of two trinuclear Ni−Gd−Ni complexes are described. The structural studies demonstrate that the two complexes present a linear arrangement of the Ni and Gd ions, with Ni ions in slightly distorted square-pyramidal or octahedral environments in complexes **1** and **2**, respectively. The Ni and Gd ions are linked by two or three phenoxo bridges, so that complexes **1** and **2** present edge-sharing or face-sharing bridging cores. Ferromagnetic interactions operate in these complexes. While a unique *J* parameter is able to fit the magnetic data of complex **2**, two very different *J* constants are needed for **1**. This result is at first sight surprising, for the structural data of the two Ni−O_2−Gd cores in complex **1** are quite similar (similar Ni−O and Gd−O bond lengths, similar angles, and dihedral angles), the only difference coming from the angle between the planes defined by the Gd ion and the two bridging phenoxo oxygen atoms of each Ni−O_2−Gd half core. This latter magnetic behavior can be considered as a signature for the participation of 5d Gd^{III} orbitals in the exchange interaction mechanism and can explain why edge-sharing complexes have larger *J* parameters than face-sharing complexes.

Introduction

The magnetic study of several Cu−Gd complexes has evidenced that ferromagnetic interactions are present in a large majority of these coordination complexes.[1,2] This property has been observed in complexes built from ligands possessing different bridges able to link the Cu and Gd ions. Among these bridging units, oxygen atoms are mainly involved, and the phenoxo bridges are the ones yielding the largest J_{Cu-Gd} interactions.[3] The accumulated experimental data have allowed a putting forward of magneto-structural correlations, the largest ferromagnetic gaps being found in planar Cu−O_2−Gd cores, with O_2 corresponding to two phenoxo bridges.[3] At variance with the magnetic properties of 3d−3d′ complexes, which are explained in terms of their orbital interactions, the mechanism responsible for the presence of general 3d-Gd ferromagnetic interaction is not as clearly documented. The first qualitative explanation was suggested by Gatteschi et al.,[4] who proposed spin polarization factors resulting from orbital interactions between the 6s Gd orbital and the 3d Cu orbitals partly delocalized on the ligand. Then, a configuration interaction based on the Good-enough model[5] and corresponding to a one-electron jump between the 3d Cu orbital and the vacant 5d Gd orbitals was advanced by Kollmar and Kahn.[6] A recent theoretical work has highlighted the active role of the ligand, evidenced the implication of 5d−4f hybridization, and demonstrated that a 5d-type atomic orbital is actually involved in the polarization scheme.[7] An even more recent work on magnetic coupling in dinuclear gadolinium complexes[8] focuses the influence of the $4f^7$−5d exchange interaction on molecular orbitals with significant 5d-orbital character to facilitate stronger ferromagnetic coupling.

Although less numerous, several examples of Ni−Ln complexes appeared in the literature.[9−24] On the basis of two structurally determined trinuclear Ni−Gd−Ni complexes

* To whom correspondence should be addressed. E-mail: costes@lcc-toulouse.fr.

(1) Benelli, C.; Gatteschi, D. *Chem. Rev.* **2002**, *102*, 2369–2387.
(2) Sakamoto, M.; Manseki, K.; Okawa, H. *Coord. Chem. Rev.* **2001**, *219−221*, 379–414.
(3) Costes, J.-P.; Dahan, F.; Dupuis, A. *Inorg. Chem.* **2000**, *39*, 165–168.
(4) Benelli, C.; Caneschi, A.; Gatteschi, D.; Guillou, O.; Pardi, L. *Inorg. Chem.* **1990**, *29*, 1750–1755.
(5) Goodenough, J. B. *Magnetism and the Chemical Bond*; Interscience: New York, 1963.
(6) Kollmar, C.; Kahn, O. *Acc. Chem. Res.* **1993**, *26*, 259–265.
(7) Paulovic, J.; Cimpoesu, F.; Ferbinteanu, M.; Hirao, K. *J. Am. Chem. Soc.* **2004**, *126*, 3321–3331.
(8) Roy, L. E.; Hughbanks, T. *J. Am. Chem. Soc.* **2006**, *128*, 568–575.
(9) Costes, J.-P.; Dahan, F.; Dupuis, A.; Laurent, J.-P. *Inorg. Chem.* **1997**, *36*, 4284–4286.
(10) Yamaguchi, T.; Sunatsuki, Y.; Kojima, M.; Akashi, H.; Tsuchimoto, M.; Re, N.; Osa; Matsumoto, S. N. *Chem. Commun.* **2004**, 1048–1049.
(11) Chen, Q.-Y.; Luo, Q.-H.; Zheng, L.-M.; Wang, Z.-L.; Chen, J.-T. *Inorg. Chem.* **2002**, *41*, 605–609.
(12) Gheorghe, R.; Andruh, M.; Costes, J. P.; Donnadieu, B.; Schmidtmann, M.; Müller, A. *Inorg. Chim. Acta* **2007**, *360*, 4044–4050.
(13) Shiga, T.; Ito, N.; Hidaka, A.; Okawa, H.; Kitagawa, S.; Ohba, M. *Inorg. Chem.* **2007**, *46*, 3492–3501.

Published on Web 04/27/2009

and their magnetic studies, we would like to give experimental evidence for the participation of 5d Gd orbitals in the magnetic interaction between nickel(II) and gadolinium (III) ions.

Experimental Section

Materials. $[L^1Ni]\cdot 1.75H_2O$,[24] (L^1: N,N′-2,2-dimethylpropylenedi(3-methoxysalicylideneiminato) ligand) and the triamine 1,1,1-tris(aminomethyl)ethane) (tame)[25] were prepared as previously described. $Gd(NO_3)_3\cdot 5H_2O$ and $Gd(CF_3SO_3)_3$ (Aldrich) were used as purchased. High-grade solvents, acetone (Normapur, VWR), methanol (Normapur, VWR), and dichloromethane, (Laboratory reagent-grade, Fisher) were used.

$[(L^1Ni(H_2O))_2Gd(H_2O)](CF_3SO_3)_3$ (1). A mixture of $[L^1Ni]\cdot 1.75H_2O$ (0.23 g, 5×10^{-4} mol) and $Gd(CF_3SO_3)_3$ (0.15 g, 2.5×10^{-4} mol) in acetone (15 mL) was stirred for 30 min and then was filtered off. The solution was concentrated to 5 mL. Addition of CH_2Cl_2 (15 mL) and stirring at room temperature yielded a green precipitate that was filtered off and dried. Yield: 0.34 g (90%). Anal. calcd for $C_{45}H_{52}F_9GdN_4Ni_2O_{19}S_3$: C, 36.2; H, 3.5; N, 3.7. Found: C, 35.8; H, 3.3; N, 3.6. Characteristic IR absorptions (KBr): 3367, 2957, 1625, 1475, 1438, 1289, 1247, 1226, 1168, 1066, 1030, 972, 851, 744, 638, 516 cm^{-1}. Mass spectrum (FAB^+, 3-nitrobenzyl alcohol matrix): m/z 1310 (20), $[(L^1Ni)_2Gd(CF_3SO_3)_2]^+$; 1161 (17), $[(L^1Ni)_2Gd(CF_3SO_3)]^+$; 882 (100), $[L^1NiGd(CF_3SO_3)_2]^+$. UV/vis: λ 632, 936 nm. Slow diffusion of dichloromethane into an acetone solution of the isolated precipitate yielded crystals suitable for an X-ray analysis.

$[(L^2Ni)_2Gd](NO_3)$ (2). To the trihydrochloride of 1,1,1-tris (aminomethyl)ethane (0.113 g, 0.5 mmol) dissolved in water (20 mL) was first added a water solution (20 mL) of NaOH (0.06 g, 1.5 mmol) followed by a dichloromethane solution (40 mL) containing o-vanillin (0.228 g, 1.5 mmol). The mixture was stirred vigorously for 2 h and was transferred into a separating funnel. The dichloromethane layer was collected and dried. The solvent was removed to yield an orange−brown oil, which was used without further purification. The oil was dissolved in dry methanol (20 mL); then, nickel acetate (0.124 g, 0.5 mmol) followed by gadolinium nitrate (0.112 g, 0.25 mmol) were added to the solution, which was stirred to give a clear solution. The filtered solution, kept undisturbed, yielded green crystals that were isolated by filtration and dried. Yield: 0.10 g (30%). Anal. calcd for $C_{58}H_{60}GdN_7Ni_2O_{15}$: C, 50.9; H, 4.4; N, 7.2. Found: C, 50.7; H, 4.3; N, 7.0. Characteristic IR absorptions (KBr), cm^{-1}: 1624, 1481, 1472, 1459, 1384, 1313, 1245, 1225, 1215, 1081, 1023, 857, 739, 641, 461. Mass spectrum (FAB^+, 3-nitrobenzyl alcohol matrix): m/z 1308 (100), $[(L^2Ni)_2Gd]^+$. UV/vis: λ 573, 980 nm.

$[(L^1Ni(H_2O))_2Y(H_2O)](H_2O)_2(CF_3SO_3)_3$ (3). This complex was made according to the experimental preparation described for **1**, with the use of $Y(CF_3SO_3)_3$ instead of $Gd(CF_3SO_3)_3$. Yield: 0.3 g (82%). Anal. calcd for $C_{45}H_{52}F_9N_4Ni_2O_{19}S_3Y$: C, 36.6; H, 4.0; N, 3.8. Found: C, 36.2; H, 4.0; N, 3.7. Characteristic IR absorptions (KBr): 3226, 2956, 1624, 1473, 1438, 1286, 1244, 1222, 1164, 1064, 1029, 968, 851, 743, 636 cm^{-1}. Mass spectrum (FAB^+, 3-nitrobenzyl alcohol matrix): m/z 1241 (22), $[(L^1Ni)_2Y(CF_3SO_3)_2]^+$; 1090 (14), $[(L^1Ni)_2Y(CF_3SO_3)]^+$; 813 (100), $[L^1NiY(CF_3SO_3)_2]^+$. UV/vis: λ 636, 957 nm.

Physical Measurements. Elemental analyses were carried out at the Laboratoire de Chimie de Coordination Microanalytical Laboratory in Toulouse, France, for C, H, and N. IR spectra were recorded on a GX system 2000 Perkin-Elmer spectrophotometer; samples were run as KBr pellets. Mass spectra (FAB^+) were recorded in DMF, used as the solvent, and a 3-nitrobenzyl alcohol matrix with a Nermag R10-10 spectrometer. Solid-state (diffuse reflectance) spectra were recorded with a Perkin-Elmer Lambda 35 UV/vis spectrometer in the 400−1100 nm range. Magnetic data were obtained with a Quantum Design MPMS SQUID susceptometer. All samples were 3-mm-diameter pellets molded from ground crystalline samples. Magnetic susceptibility measurements were performed in the 2−300 K temperature range in a 0.1 T applied magnetic field, and diamagnetic corrections were applied using Pascal's constants.[26] Isothermal magnetization measurements were performed up to 5 T at 2 K. The magnetic susceptibilities have been computed by exact calculations of the energy levels associated with the spin Hamiltonian through diagonalization of the full matrix with a general program for axial symmetry,[27] and with the MAGPACK program package.[28] Least-squares fittings were accomplished with an adapted version of the function-minimization program MINUIT.[29]

Crystallographic Data Collection and Structure Determination for 1 and 2. Crystals of **1** and **2** were kept in the mother liquor until they were dipped into oil. The chosen crystals were mounted on a Mitegen micromount and quickly cooled down to 180 K. The selected crystals of **1** (green, $0.35 \times 0.22 \times 0.08$ mm^3) and **2** (light green, $0.45 \times 0.05 \times 0.025$ mm^3) were mounted on an Oxford-Diffraction XCALIBUR machine (**1** and **2**) using a graphite monochromator ($\lambda = 0.71073$ Å) and equipped with an Oxford Cryosystems cooler device. The data were collected at 180 K (**1** and **2**). The unit cell determination and data integration were carried out using the CrysAlis RED package.[30] A total of 49 443 reflections were collected for **1**, of which 13 089 were independent (Rint = 0.0437), and 70 222 reflections for **2**, of which 19 602 were independent (Rint = 0.1602). The structures have been solved by direct methods using SIR92[31] and refined by least-squares procedures on F^2 with the program SHELXL97,[32] included in the software

(14) Pointillart, F.; Bernot, F.; Sessoli, R.; Gatteschi, D. *Chem.—Eur. J.* **2007**, *13*, 1602–1609.
(15) Lisowski, J.; Starynowicz, P. *Inorg. Chem.* **1999**, *38*, 1351–1355.
(16) Xu, Z.; Read, P. W.; Hibbs, D. E.; Hursthouse, M. B.; Malik, K. M. A.; Rettig, S. J.; Seid, M.; Summers, D. A.; Pink, M.; Thompson, R. C.; Orvig, C. *Inorg. Chem.* **2000**, *39*, 508–516.
(17) Bayly, S. R.; Xu, Z.; Patrick, B. O.; Rettig, S. J.; Pink, M.; Thompson, R. C.; Orvig, C. *Inorg. Chem.* **2003**, *42*, 1576–1583.
(18) Kahn, M. L.; Lecante, P.; Verelst, M.; Mathonière, C.; Kahn, O. *Chem. Mater.* **2000**, *12*, 3073–3079.
(19) Yue, Q.; Yang, J.; Li, G.-H.; Li, G.-D.; Xu, W.; Chen, J. S.; Wang, S. N. *Inorg. Chem.* **2005**, *44*, 5241–5246.
(20) Ouyang, Y.; Zhang, W.; Xu, N.; Xu, G. F.; Liao, D. Z.; Yoshimura, K.; Yan, S. P.; Cheng, P. *Inorg. Chem.* **2007**, *46*, 8454–8456.
(21) Gao, H. L.; Yi, L.; Wang, H. S.; Cheng, P.; Liao, D. Z.; Yan, S. P. *Inorg. Chem.* **2006**, *45*, 481–483.
(22) Barta, C. A.; Bayly, S. R.; Read, P. W.; Patrick, B. O.; Thompson, R. C.; Orvig, C. *Inorg. Chem.* **2008**, *47*, 2280–2293.
(23) Chandrasekhar, V.; Murugesa Pandian, B.; Boomishankar, R.; Steiner, A.; Vittal, J. J.; Houri, A.; Clérac, R. *Inorg. Chem.* **2008**, *47*, 4918–4929.
(24) Costes, J. P.; Donnadieu, B.; Gheorghe, R.; Novitchi, G.; Tuchagues, J. P.; Vendier, L. *Eur. J. Inorg. Chem.* **2008**, 5235–5244.
(25) Fleischer, E. B.; Gebala, A. E.; Levey, A.; Tasker, P. A. *J. Org. Chem.* **1971**, *36*, 3042–3044.
(26) Pascal, P. *Ann. Chim. Phys.* **1910**, *19*, 5–70.
(27) Boudalis, A. K.; Clemente-Juan, J.-M.; Dahan, F.; Tuchagues, J.-P. *Inorg. Chem.* **2004**, *43*, 1574–1586.
(28) Borrás-Almenar, J. J.; Clemente-Juan, J. M.; Coronado, E.; Tsukerblat, B. S. *Inorg. Chem.* **1999**, *38*, 6081–6088. Borrás-Almenar, J. J.; Clemente-Juan, J. M.; Coronado, E.; Tsukerblat, B. S. *J. Comput. Chem.* **2001**, *22*, 985–991.
(29) James, F.; Roos, M. *Comput. Phys. Commun.* **1975**, *10*, 343–367.
(30) *CrysAlis RED*, version 1.170.32; Oxford Diffraction Ltd.: Oxfordshire, U.K., 2003.
(31) SIR92 − a program for crystal structure solution: Altomare, A.; Cascarano, G.; Giacovazzo, C.; Guagliardi, A. *J. Appl. Crystallogr.* 1993, 26, 343−350.
(32) Sheldrick, G. M. *SHELX97* [includes SHELXS97, SHELXL97, CIFTAB], release 97−2; Institüt für Anorganische Chemie der Universität: Göttingen, Germany, 1998.

Table 1. Crystallographic Data for Complexes **1** and **2**

	1	**2**
formula	$C_{47}H_{58}Cl_4F_9GdN_4Ni_2O_{20}S_3$	$C_{58}H_{60}GdN_7Ni_2O_{15}$
fw	1682.62	1369.76
space group	$P2_1/c$	$C2/c$
a, Å	16.8541(3)	47.138(6)
b, Å	16.2088(3)	24.506(3)
c, Å	24.2499(5)	17.806(3)
α, deg	90	90
β, deg	104.645(2)	110.96(1)
γ, deg	90	90
V, Å^{-3}	6409.5(2)	19208(5)
Z	4	12
ρ_{calcd}, g cm^{-3}	1.744	1.421
λ, Å	0.71073	0.71073
T, K	180(2)	180
μ(Mo Kα), mm^{-1}	1.967	1.672
R^a obs, all	0.0325, 0.0642	0.0660, 0.1775
Rw^b obs, all	0.0751, 0.0902	0.1268, 0.1575

$^a R = \sum||F_o| - |F_c||/\sum|F_o|$. $^b wR_2 = [\sum w(|F_o^2| - |F_c^2|)^2/\sum w|F_o^2|^2]^{1/2}$.

package WinGX, version 1.63.[33] The atomic scattering factors were taken from the International Tables for X-ray Crystallography.[34] All hydrogen atoms were geometrically placed and refined with a riding model. All non-hydrogens atoms were anisotropically refined, and in the last cycles of refinement, a weighting scheme was used, where weights are calculated from the following formula: $w = 1/[\sigma^2(F_o^2) + (aP)^2 + bP]$, where $P = (F_o^2 + 2F_c^2)/3$. It was not possible to solve diffuse electron-density residuals (enclosed solvent molecules) for complex **2**. Treatment with the SQUEEZE facility from PLATON[35] resulted in a smooth refinement. Since a few low-order reflections are missing from the data set, the electron count is underestimated. Thus, for complex **2**, the values given for D(calc), F(000), and the molecular weight are only valid for the ordered part of the structure. Drawings of molecules are performed with the program Cameron[36] with 30% probability displacement ellipsoids for non-hydrogen atoms. It was not possible to resolve diffuse electron-density residuals (enclosed solvent molecule) for complex **2**. Treatment with the SQUEEZE facility from PLATON[37] resulted in a smooth refinement. Since a few low-order reflections are missing from the data set, the electron count will be underestimated. Thus, the values given for D(calc), F(000), and the molecular weight are only valid for the ordered part of the structure.

Results

The two nickel−gadolinium complexes crystallize in monoclinic space groups, $P2_1/n$ for **1** with $Z = 4$ and $C2/c$ for **2** with $Z = 12$. The crystallographic data of the two complexes appear in Table 1, while selected bond lengths and angles are collected in the figure captions. The structural determination of complex **1** evidences the existence of a trinuclear cationic Ni−Gd−Ni complex, as shown in Figure 1. The formula of the cation is $[(L^1NiH_2O)_2GdH_2O]^{3+}$. A water molecule is linked to each metal ion, while the three triflate anions act as conterions. The gadolinium center is nine-coordinate to the four phenoxo and the four

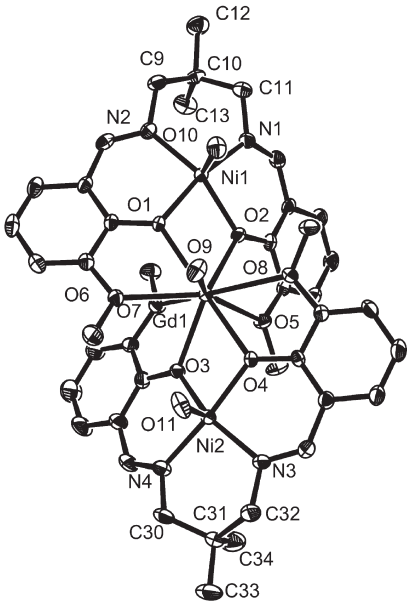

Figure 1. Cameron plot of complex **1** at the 30% probability level. H atoms and noncoordinated triflate anions have been omitted for clarity. Selected bond lengths (Å) and angles (deg) for the $[(L^1Ni(H_2O))_2Gd(H_2O)]^{3+}$ cation: O(1)−Ni(1) 1.980(3), O(2)−Ni(1) 2.042(2), N(1)−Ni(1) 1.999(3), N(2)−Ni(1) 2.002(3), O(10)−Ni(1) 2.008(3), O(1)−Gd(1) 2.405(2), O(2)−Gd(1) 2.337(2), O(5)−Gd(1) 2.538(2), O(6)−Gd(1) 2.594(2), O(2)−Ni(1)−O(1) 77.1(1), Ni(1)−O(1)−Gd(1) 107.3(1), Ni(1)−O(2)−Gd(1) 107.7(1), O(2)−Gd(1)−O(1) 63.82(8). For the L^1Ni (2) unit: O(3)−Ni(2) 2.005(2), O(4)−Ni(2) 1.987(2), N(3)−Ni(2) 1.998(2), N(4)−Ni(2) 1.992(3), O(11)−Ni(2) 1.988(3), O(3)−Gd(1) 2.336(2), O(4)−Gd(1) 2.389(2), O(7)−Gd(1) 2.528(3), O(8)−Gd(1) 2.577(3), O(9)−Gd(1) 2.307(3), O(4)−Ni(2)−O(3) 76.6(1), Ni(2)−O(3)−Gd(1) 108.2(1), Ni(2)−O(4)−Gd(1) 106.9(1), O(4)−Gd(1)−O(3) 63.15(8).

methoxy oxygen atoms of the two L^1 ligands and to a water molecule. Surprisingly, the nickel ions are five-coordinate to the N_2O_2 coordination site of the ligand and to a water molecule in the axial position. The lanthanide complexation induces a change into the six-membered diamino ring from a twist-boat to a chair conformation.[38] The L^1Ni moieties are not planar; they take an umbrella form with the water molecule pointing above. The related Ni···Gd separations are equal to 3.539(1) Å and 3.523(1) Å. The angle between the two OGdO planes containing the phenoxo oxygen atoms is equal to 62.3(1)°, and the dihedral angles between the Ni1O1O2 and GdO1O2 and the Ni2O3O4 and GdO3O4 planes are equal to 18.5(1) and 20.5(1)°, respectively. Nevertheless, the Ni···Gd···Ni centers are aligned, with a Ni···Gd···Ni angle of 179.0(1)°. Although hydrogen bonds involving the water molecules and the noncoordinated triflate anions are present, the different trinuclear units are well-isolated from each other, with Ni···Ni and Ni···Gd distances larger than 8.3 Å.

The complex $[L^2NiGdNiL^2](NO_3)$ crystallizes in the $C2/c$ centrosymmetric space group with $Z = 12$. The screw arrangement of the achiral tripodal ligand around the 3d ion yields chiral Λ or Δ configurations, and the assembling of two chiral molecules by the Ln ion can result in homochiral (Λ−Λ or Δ−Δ) and heterochiral (Λ−Δ) pairs. The centrosymmetric space group clearly indicates that we are dealing with a racemic crystal, where Λ−Λ and Δ−Δ pairs coexist,

(33) WINGX - 1.63 Integrated System of Windows Programs for the Solution, Refinement and Analysis of Single Crystal X-Ray Diffraction Data: Farrugia, L. *J. Appl. Crystallogr.* 1999, 32, 837−838.
(34) *International Tables for X-Ray Crystallography*; Kynoch Press, Birmingham, England, 1974; Vol. IV.
(35) SQUEEZE: Sluis, P. V.D.; Spek, A. L. *Acta Crystallogr.* 1990, A46, 194−201.
(36) CAMERON: Watkin, D. J.; Prout, C. K.; Pearce, L. J. *Chemical Crystallography Laboratory*; University of Oxford, Oxford, 1996.
(37) Sluis, P. V. D.; Spek, A. L. *Acta Crystallogr.* **1990**, *A46*, 194–201.
(38) Costes, J. P.; Donnadieu, B.; Gheorghe, R.; Novitchi, G.; Tuchagues, J. P.; Vendier, L. *Eur. J. Inorg. Chem.* **2008**, 5235–5244.

while the heterochiral (Λ−Δ) pairs are absent. Furthermore, the asymmetric unit contains two different $[L^2NiGdNiL^2]^+$ cationic entities. The first one (Figure 2) possesses two slightly different nickel environments, while the second one is symmetry-related through the Gd ion, which results in $Z = 12$. In the nonsymmetrical entity, the Ni−O bonds are equal at average values of 2.056 and 2.066 Å. An average value of 2.054 Å is observed for the symmetrical one. These two entities still correspond to linear trinuclear complexes, with similar Ni···Gd···Ni angles (178.41(5)° and 178.68(5)°) and slightly different Ni···Gd distances (3.321(1) Å for the symmetric unit against 3.305(1) and 3.313(1) Å for the other one). The Gd−O bonds of the two units are quite similar, including the deprotonated phenoxo oxygens with bond lengths varying from 2.373(6) to 2.434(6) Å and the neutral methoxy oxygens characterized by larger bond lengths, from 2.877(6) to 2.950(6) Å. There are no hydrogen bonds between adjacent trinuclear complexes, and the shortest Ni···Ni distances are around or larger than 8 Å, implying that the trinuclear complexes may be considered to be well-isolated

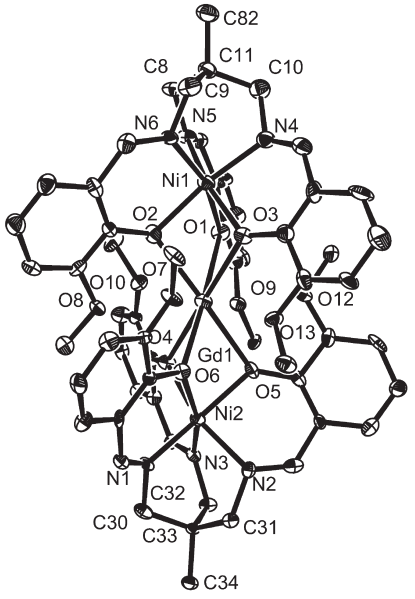

Figure 2. Cameron plot of complex **2** at the 30% probability level. H atoms have been omitted for clarity. Selected bond lengths (Å) and angles (deg) for the nonsymmetric $[(L^2Ni)_2Gd]^+$ cation: O(1)−Ni(1) 2.065(6), O(2)−Ni(1) 2.063(6), O(3)−Ni(1) 2.041(6), N(4)−Ni(1) 2.053(8), N(5)−Ni-(1) 2.050(7), N(6)−Ni(1) 2.062(8), O(4)−Ni(2) 2.066(6), O(5)−Ni(2) 2.048(6), O(6)−Ni(2) 2.085(6), N(1)−Ni(2) 2.005(7), N(2)−Ni(2) 2.077 (7), N(3)−Ni(2) 2.077(8), O(1)−Gd(1) 2.374(6), O(2)−Gd(1) 2.380(6), O(3)−Gd(1) 2.430(6), O(4)−Gd(1) 2.405(6), O(5)−Gd(1) 2.391(6), O(6)−Gd(1) 2.373(6), O(7)−Gd(1) 2.893(6), O(8)−Gd(1) 2.973(6), O(9)−Gd(1) 2.907(6), O(10)−Gd(1) 2.884(6), O(12)−Gd(1) 2.901(6), O(13)−Gd(1) 2.877(6), O(2)−Ni(1)−O(1) 76.8(2), O(3)−Ni(1)−O(1) 76.7(2), O(2)−Ni-(1)−O(3) 78.4(3), Ni(1)−O(1)−Gd(1) 96.0(2), Ni(1)−O(2)−Gd(1) 95.9 (2), Ni(1)−O(3)−Gd(1) 94.9(3), O(2)−Gd(1)−O(1) 65.3(2), O(2)−Gd-(1)−O(3) 65.2(2), O(3)−Gd(1)−O(1) 64.0(2), O(4)−Ni(2)−O(5) 77.4(2), O(4)−Ni(2)−O(6) 77.2(2), O(5)−Ni(2)−O(6) 76.0(2), Ni(2)−O(4)−Gd-(1) 95.3(2), Ni(2)−O(5)−Gd(1) 96.2(2), Ni(2)−O(6)−Gd(1) 95.8(2), O(4)−Gd(1)−O(5) 64.9(2), O(4)−Gd(1)−O(6) 65.6(2), O(5)−Gd(1)−O(6) 64.6(2). For the symmetric cation: O(15)−Ni(3) 2.060(6), O(17)−Ni(3) 2.051(6), O(18)−Ni(3) 2.051(6), N(7)−Ni(3) 2.077(8), N(8)−Ni(3) 2.059(8), N(9)−Ni(3) 2.031(8), O(14)−Gd(2) 2.950(6), O(15)−Gd(2) 2.393(6), O(16)−Gd(2) 2.877(6), O(17)−Gd(2) 2.434(6), O(18)−Gd(2) 2.428(6), O(19)−Gd(2) 2.946(6), Ni(3)−O(15)−Gd(2) 96.2(2), Ni(3)−O-(17)−Gd(2) 95.2(2), Ni(3)−O(18)−Gd(2) 95.4(2), O(15)−Ni(3)−O(17) 77.7(2), O(15)−Ni(3)−O(18) 78.5(2), O(17)−Ni(3)−O(18) 77.0(3), O-(15)−Gd(2)−O(17) 64.6(2), O(15)−Gd(2)−O(18) 65.3(2), O(17)−Gd-(2)−O(18) 63.4(2).

from each other. The coordination geometry around each Ni metal ion is distorted from a regular octahedron. This deformation is easily analyzed with the "SHAPE" program.[39] The nickel environments in the symmetrical and nonsymmetrical $[L^2NiGdNiL^2]$ units can be considered distorted octahedrons, the distortion being larger in the nonsymmetrical unit (3.35 and 3.52) in comparison to the symmetrical one (2.45). These distortions correspond to the Bailar trigonal twist, for the Bailar-twist symmetry constant found for our complex (4.3) does not depart from the value expected for a pure Bailar-twist route (4.2).[40] Analysis of the pentacoordinate Ni polyhedra in complex **1** indicates that the geometry around the Ni centers is closer to square-pyramid (1.12 and 1.40 for Ni1 and Ni2, respectively) than to vacant octahedron (1.61 and 1.58).

Magnetic Data. The magnetic susceptibilities of the Ni−Gd−Ni complexes **1** and **2** have been measured in the 300−2 K temperature range with an applied magnetic field of 0.1 T. As the magnetic behavior of complex **2** is simpler, it will be studied first. The thermal variation of the $\chi_M T$ product for complex **2** is represented in Figure 3, χ_M being the molar magnetic susceptibility of the trinuclear species corrected for the diamagnetism of the ligands. At 300 K, $\chi_M T$ is equal to 9.70 cm^3 K mol^{-1} and corresponds to what is expected for two nickel and one gadolinium ions without magnetic interaction (9.87 cm^3 mol^{-1} K with $g = 2.0$ for Ni ions). Lowering the temperature results initially in a smooth increase of $\chi_M T$ (10.26 cm^3 K mol^{-1} at 40 K) and then in a steeper increase, up to 14.87 cm^3 K mol^{-1} at 2 K. A quantitative analysis has been performed on the basis of an expression derived from the following Hamiltonian:

$$H = -J_{NiGd}(S_{Ni_1}S_{Gd} + S_{Ni2}S_{Gd}) + D(S_z^2Ni1 + S_z^2Ni2)$$

in which the first term gauged by the parameter J accounts for the spin exchange interaction and the second one gauged by D accounts for axial single-ion zero-field splitting (ZFS) of nickel(II) ions. This Hamiltonian takes into consideration the structural characteristics of complex **2**, with two equivalent Ni_1−Gd and Ni_2−Gd exchange interactions J and two identical ZFS terms D. Using exact diagonalization of the energy matrix for an $S_1 = 1$, $S_2 = 7/2$, $S_3 = 1$ trinuclear system, the best fit shown in Figure 3 yields the following parameters, $J_{NiGd} = 0.91$ cm^{-1}, $g = 1.98$, and $D = 4.5$ cm^{-1} and an agreement factor R of 3.3×10^{-5}, where $R = \sum[(\chi_M T)_{obs} - (\chi_M T)_{calcd}]^2/\sum[(\chi_M T)_{obs}]^2$. The magnetization measurements in the 0−5 T range at 2 K that are satisfactorily simulated with

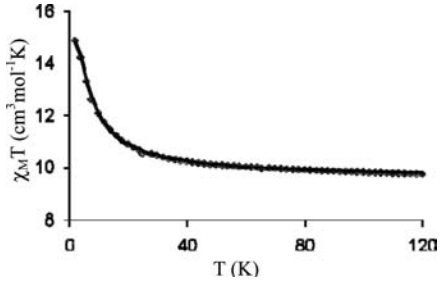

Figure 3. Thermal variation of the $\chi_M T$ product for complex **2**. The full line corresponds to the best fit to the experimental data (see text).

this set of parameters (Figure 4, diamonds and solid line) do confirm an $S = 11/2$ ground state, with an M value of 10.5 Nβ units at 5 T.

At first sight, the thermal behavior of the $\chi_M T$ product for complex **1**, represented in Figure 5, looks like that observed for complex **2**. At 300 K, $\chi_M T$ is equal to 10.38 cm^3 K mol^{-1}, which is slightly larger than expected for two nickel and one gadolinium ion without magnetic interaction (10.1 cm^3 mol^{-1}K with $g = 2.1$ for Ni ions). Lowering the temperature results in a slightly more rapid $\chi_M T$ increase (10.99 cm^3 K mol^{-1} at 100 K), while the final $\chi_M T$ value at 2 K is lower (14.13 cm^3 K mol^{-1}) than for complex **2**. Surprisingly, the above Hamiltonian corresponding to a trinuclear Ni−Gd−Ni model of two nickel ions interacting with a gadolinium ion and unique J_{NiGd} and D_{Ni} parameters is not able to fit the experimental data in the 300−10 K region of the $\chi_M T$ product (Figure S1, Supporting Information). Because in this temperature domain the $\chi_M T$ experimental data are mainly sensitive to the J parameter, we decided to use a Hamiltonian including two different J parameters. Furthermore, in view of the structural determination, we kept an equivalent D term for both nickel ions, in order to avoid overparametrization. Surprisingly, the corresponding spin Hamiltonian allows a nice fit of the experimental data over the entire temperature range.

$$H = -J_{NiGd}(S_{Ni_1} S_{Gd}) - j_{NiGd}(S_{Ni2} S_{Gd}) + D(S_z^2 Ni1 + S_z^2 Ni2)$$

The best fit, shown in Figure 5, yields the following parameters: $J_{NiGd} = 4.8(3)$ cm^{-1}, $j_{NiGd} = 0.05(2)$ cm^{-1}, $g = 2.03(1)$, and $D = 0.03(1)$ cm^{-1} and an agreement factor R of 1×10^{-5}. In view of the small D parameter value, an equivalent fit may be obtained for D values

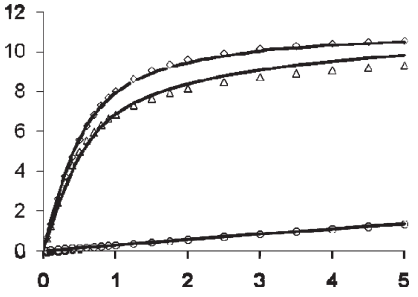

Figure 4. Field-dependent magnetization of complexes **1** (triangles), **2** (diamonds), and **3** (circles) at 2 K. The solid lines correspond to the Brilloin functions for the parameters extracted from the static susceptibility and magnetization data (see text).

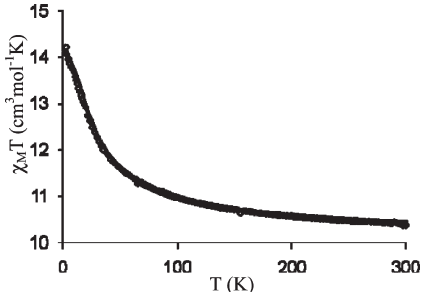

Figure 5. Thermal variation of the $\chi_M T$ product for complex **1**. The full line corresponds to the best fit to the experimental data (see text).

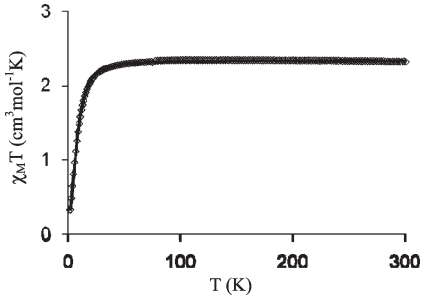

Figure 6. Thermal variation of the $\chi_M T$ product for complex **3**. The full line corresponds to the best fit to the experimental data (see text).

equal to zero, without significant variations of the J and g parameters. It has to be noted that the 300−7 K temperature range fitted without j and D parameters yields a very similar J value (5.0 cm^{-1}). The magnetization value M increases up to 9.3 Nβ at 5 T (Figure 4, triangles), not far from what is expected for an $S = 9/2$ ground state, corresponding to a ferromagnetic coupling between one Ni^{II} and one Gd^{III} ion. The presence of the second Ni^{II} ion behaving at least as a paramagnetic ion should give an M value around 11 Nβ units. The observed M value of 9.3 Nβ at 5 T can only be explained if anisotropy is present in **1**. In order to check this hypothesis, the corresponding isostructural Ni−Y−Ni complex **3** has been prepared. The magnetic study confirms that the magnetic behavior can be correctly fitted (Figure 6) with use of a unique D term ($D = 19.7$ cm^{-1}, $g_{Ni} = 2.16$, $R = 2 \times 10^{-5}$), in perfect agreement with a recent study on pentacoordinate Ni^{II} complexes.[41] The magnetization curve corresponding to complex **3** is also reported in Figure 4 (circles), where we can see that the contribution of two nickel ions is lower than the expected value in the absence of ZFS (1.36 instead of 4 Nβ). The best fit of these experimental magnetization data with Magpack yielded a D value of 19.8 cm^{-1}. Taking these results into account, an approximate fit of the magnetization curve with $J = 5$ cm^{-1}, $j = 0$, $D = 12.4$ cm^{-1}, $g_{Ni} = 2.16$, and $g_{Gd} = 2.00$ has been obtained, as reported in Figure 4 (solid line and triangles). These data confirm that the simplified model for complex **1**, considered as a ferromagnetic Ni−Gd dinuclear unit plus a mononuclear pentacoordinate Ni ion having a large magnetic anisotropy due to zero-field splitting, does agree with the low experimental magnetization value of 9.3 Nβ at 5 T.

From the entire set of data obtained for **1**, it becomes clear that a correlation between the j_{NiGd} and D terms does exist in that complex. We must recall that these terms play an important role in the low-temperature range (8−2 K), so that the influence of the anisotropic term D is best reproduced by the magnetization curve at 2 K. At variance, the lower j_{NiGd} and D values are retained in the fit of the $\chi_M T$ product, where the larger J_{NiGd} parameter holds the main role. Indeed, a fit with a D term kept to a constant value of 12 cm^{-1} (Figure S2, Supporting

(39) Alvarez, S.; Avnir, D.; Llunell, M.; Pinsky, M. *New J. Chem.* **2002**, *26*, 996–1009.
(40) Bailar, J. C.Jr. *J. Inorg. Nucl. Chem.* **1958**, *8*, 165–175.
(41) Rebilly, J. N.; Charron, G.; Rivière, E.; Guillot, R.; Barra, A. L.; Duran Serrano, M.; van Slageren, J.; Mallah, T. *Chem.—Eur. J.* **2008**, *14*, 1169–1177.

Information) yields a parameter j_{NiGd} equal to 0.34 cm^{-1} with a nice R factor of 4×10^{-5}.

Discussion

Although complexes **1** and **2** studied in this work correspond to trinuclear Ni−Gd−Ni entities with a linear arrangement of the three metal ions, they present several different characteristics. First, from the structural point of view, the nickel ions involved in the two trinuclear Ni−Gd−Ni complexes have different coordination spheres, distorted octahedrons for complex **2** and square-pyramids for complex **1**. The second difference originates from the bridging Ni−Gd units. The edge-sharing complex **1** possesses two phenoxo bridges linking the Ni and Gd ions, while the face-sharing complex **2** has three phenoxo bridges linking the Ni and Gd ions. Then, although ferromagnetic Ni−Gd interactions operate in both complexes, these trinuclear entities can be considered as having different global magnetic behaviors, which is the main purpose of this work.

The mechanism of ferromagnetic coupling in copper−gadolinium complexes has been recently approached from a theoretical point of view.[7] The authors concluded that the qualitative model of Kollmar and Kahn,[6] based on the configuration interaction model of Goodenough,[5] and assigned to the electron jump from 3d Cu^{II} orbitals to 5d Gd^{III} orbitals, can be partly responsible for the existence of this phenomenon. They also showed that the ligand plays an active role in magnifying the ferromagnetic coupling by spin polarization effects, as previously described by Gatteschi and co-workers,[4] who assumed the role of 6s Gd^{III} atomic orbitals in the polarization scheme. From their quantum chemical calculations, these authors found that one 5d-type Gd^{III} atomic orbital is involved in this polarization scheme. Within the C_{2v} symmetry, their results show that the system adopts an orthogonal orbital exchange pathway, with the main interaction operating between $b_2[Cu^{II}L]$ and $a_2[Gd^{III}]$ orbitals, responsible for ferromagnetic coupling.

The room-temperature $\chi_M T$ product of **1** clearly indicates that the two nickel ions are in the high-spin state, while the structural determination evidences that they are both bridged to the gadolinium ion. Although the structural data of the two Ni−O_2−Gd cores are quite similar (similar Ni−O and Gd−O bond lengths, similar angles and dihedral angles (20.5(8) and 18.5(8)°)), fitting the magnetic data requires using two different interaction parameters, J_{NiGd} and j_{NiGd}. This result is at first sight surprising, particularly in view of these structural parameters. If we remember that the strength of the magnetic interaction in Cu−Gd complexes is correlated to the value of the dihedral angle between the two halves of the Cu−O_2−Gd bridging core,[3] the structural data observed for complex **1** (dihedral angles (20.5(8) and 18.5(8)°)) should be associated to J values close to each other. At variance with this rationale, fitting the magnetic data yields quite different J parameters, 4.8 and 0.05 cm^{-1}. A closer look at complex **1** shows that the two L^1Ni entities are not symmetrically arranged around the Gd ion. Indeed, although the Ni···Gd···Ni centers are linearly arranged, with a Ni···Gd···Ni angle of 179.0(1)°, the angle between the planes defined by the Gd ion and the two bridging phenoxo oxygen atoms of each Ni−O_2−Gd half core is equal to 62.3(1)°. In order to explain the presence of two different interaction parameters J and j, we are led to conclude that orthogonality of the 3d−5d orbitals present in one of the Ni−O_2−Gd half cores of **1** prevents a similar orthogonal orbital arrangement in the other Ni−O_2−Gd half core, as a consequence of the different orientations of the 3d Ni^{II} orbitals with regard to the 5d Gd^{III} orbitals. An increased overlap favoring the antiferromagnetic contributions is consistent with a weakening of the ferromagnetic coupling and explains the operation of two different interaction parameters, J and j in **1**.[42] This behavior implies that the 5d Gd^{III} orbitals do participate in the exchange interactions, but not the 6s Gd^{III} orbital, which is spherical and thus insensitive to a geometrical factor. This experimental observation is in complete agreement with the theoretical work previously published.[7]

Till now, the largest J value found in a heterodinuclear Ni−Gd complex was equal to 3.6 cm^{-1},[9] implying that ~2 cm^{-1} may be expected as the highest J value for a trinuclear Ni−Gd−Ni entity with two active and equivalent Ni−Gd interactions. Considering that the fit yields a J value of 4.8 cm^{-1} for one Ni−Gd interaction in the trinuclear complex **1**, it is expected that the second Ni−Gd interaction is inefficient and characterized by a value close to zero. From the entire set of data obtained for **1**, it becomes clear that a correlation between j_{NiGd} and D terms does exist in this complex. We must recall that these terms play a role in the low-temperature range (8−2 K). Unfortunately, the lower j_{NiGd} and D values are retained when fitting the $\chi_M T$ product, where the larger J_{NiGd} parameter holds the main role. Nevertheless, a fit with a D term kept to a constant value of 12 cm^{-1} yields a parameter j_{NiGd} equal to 0.34 cm^{-1} with a correct R factor of 4×10^{-5} (Figure S2, Supporting Information).

On the contrary, the prominent role of the anisotropy term D is best evidenced by the magnetization curves at 2 K for complexes **1**, **2**, and **3**. The magnetization for **2** (10.5 Nβ) at 5 T is not far from the value expected for a trinuclear Ni−Gd−Ni complex with an $S = 11/2$ ground state, confirming operation of the ferromagnetic interactions between each Ni^{II} ion and the central Gd^{III} ion (Figure 4, diamonds). At variance, the lower M value and the positive M versus H slope observed for **1** indicate that saturation is not reached. In view of the different J and j parameters, complex **1** can be sketched at the limit as a dinuclear Ni−Gd unit associated with a mononuclear Ni ion, the latter experiencing significant anisotropy (Figure 4, triangles). This magnetic anisotropy, due to the pentacoordination of the nickel ion, is responsible for the low magnetization value found in complex **3**, 1.36 Nβ for two nickel ions (Figure 4, circles). A magnetization value around 9 Nβ units is expected for a ferromagnetic dinuclear Ni−Gd entity without ZFS.[9] Adding the contribution of an anisotropic nickel ion as in complex **3** to the contribution of a ferromagnetic Ni−Gd entity must yield a value close to the experimental value of 9.3 Nβ found for **1** at 5 T. This magnetization value appears to be a sound argument for the presence of largely different ferromagnetic interaction parameters in complex **1**.

Comparison of a trinuclear Ni−Gd−Ni complex[10] derived from the tripodal ligand 1,1,1-tris[(salicylideneamino) methyl]ethane with complex **2** evidences the advantage of the present tripodal bridging ligand. In the absence of methoxy substituents in the α position of the phenoxo bridges, the assembling of two anionic nickel−ligand entities by a gadolinium ion results in the presence of only six oxygen

(42) Kahn, O. *Molecular Magnetism*; VCH: Weinheim, Germany, 1993.

atoms in the Gd coordination sphere, leaving enough room for a chelating nitrato anion to bind the 4f ion. The NO_3 chelation induces a misalignment of the Ni−Gd−Ni ions, characterized by a bent Ni···Gd···Ni core and an angle of ∼140°.[10] Using the NiL^2 entity, based on ortho-vanillin instead of salicylaldehyde, 12 oxygen atoms enter the Gd coordination sphere, repelling the anionic nitrate out of the Gd coordination sphere and yielding a practically linear Ni−Gd−Ni complex (Ni···Gd···Ni angle of 178.5(1)°). This geometric difference is responsible for a 5-fold increase of the magnetic interaction, from 0.19 to 0.91 cm^{-1} for complex **2**. A participation of the 5d Gd^{III} orbital may be again argued for explaining this *J* increase, the higher symmetry corresponding to the better orthogonality.

In a face-sharing complex such as **2**, both $d_{x^2-y^2}$ and d_{z^2} orbitals of nickel ions are involved in bridging. This situation is more favorable to an overlap between the 3d Ni orbitals and the 5d Gd orbitals through the phenoxo bridges and would explain why the *J* values are lower in face-sharing compared to edge-sharing complexes. It is clear that orbital orthogonality is easier to reach when the $d_{x^2-y^2}$ orbitals are the only ones involved.

Conclusion

The present work highlights the participation of the 5d Gd^{III} orbitals, or at least one of them, in the magnetic interactions in Ni−Gd complexes. Such an involvement, previously proposed in a theoretical study aimed at explaining the mechanism of ferromagnetic coupling in Cu−Gd complexes,[7] is supported by the fact that two interaction parameters are required in order to fit the magnetic data obtained for the trinuclear Ni−Gd−Ni complex **1**. The structural determination indicates that the OGdO planes containing the bridging phenoxo oxygen atoms involved in the two Ni−O_2−Gd half cores of **1** make an angle of 62.3(1)°. The Ni−Gd−Ni molecule being linear and the two Ni−Gd parts of the core having very similar geometric parameters implies that the orbital orthogonality cannot be reached simultaneously by both Ni−Gd parts of the core. A different orbital overlap in each Ni−Gd part of the core through the phenoxo bridges justifies the use of two coupling constants. Furthermore, with the interaction parameter being larger for one of the Ni−Gd units of **1**, as in a dinuclear Ni−Gd complex,[9] than in complex **2**, of pseudo-C_3 symmetry, it seems reasonable to suggest that the Ni−Gd contacts responsible for orbital orthogonality are more efficient when the concerned orbitals are involved in edge-sharing complexes. Until now, the larger *J* parameters (coupling constants) have been found for complexes that possess edge-sharing 3d-bridging atoms and Gd cores, in Cu−Gd or Ni−Gd complexes, the largest ones being observed for complexes including two phenoxo bridges.[3,9] The present work evidences that ferromagnetic interactions are not related to the approximate pseudo-C_{2v} geometry of the large majority of the Cu−Ln complexes published until now.[7] These ferromagnetic interactions may be considered as a genuine property of the 3d-Gd complexes. Indeed, complex **2**, which is characterized by a symmetry different from C_{2v}, is still governed by ferromagnetic interactions. It has been observed in previous work that the main factor responsible for the variation of the *J* interaction parameter is the dihedral angle between the planes defining the two halves (OMO and OGdO) of the M−O_2−Gd core.[3] A similar observation has also been made for nonsymmetrical bridges.[43,44] Involvement of the 6s Gd orbital would not be sensitive to geometrical factors, while participation of at least one 5d orbital can easily explain such behavior. We hope that these experimental results will generate new theoretical calculations that will provide a better view of the magnetic interactions involved in 3d−4f complexes.

Acknowledgment. This work was supported by the European Union sixth framework program NMP3-CT-2005-515767 entitled "MAGMANet: Molecular Approach to Nanomagnets and Multifunctional Materials". The authors are grateful to Dr. A. Mari and Ms. S. Seyrac for technical assistance and to Dr. Juan-Modesto Clemente Juan for helpful discussions.

Supporting Information Available: X-ray crystallographic file in CIF format for **1** and **2**, Figures S1 and S2 reporting simulations of magnetic data. This material is available free of charge via the Internet at http://pubs.acs.org.

(43) Costes, J.-P.; Dahan, F.; Dupuis, A.; Laurent, J.-P. *Inorg. Chem.* **2000**, *39*, 169–173.
(44) Chiboub Fellah, F. Z.; Costes, J. P.; Dahan, F.; Duhayon, C.; Novitchi, G.; Tuchagues, J. P.; Vendier, L. *Inorg. Chem.* **2008**, *47*, 6444–6451.